2011-07-13

Mapping and Modeling Chlorophyll-a Concentrations in Utah Lake Using Landsat 7 ETM+ Imagery

Victor Nii Afum Narteh
Brigham Young University - Provo

Mapping and Modeling Chlorophyll-*a* Concentrations in Utah Lake

Using Landsat 7 ETM+ Imagery

Victor Nii Afum Narteh

A thesis submitted to the faculty of
Brigham Young University
in partial fulfillment of the requirements for the degree of

Master of Science

M. Brett Borup, Chair
Gustavious P. Williams
A. Woodruff Miller

Department of Civil & Environmental Engineering

Brigham Young University

August 2011

ABSTRACT

Mapping and Modeling Chlorophyll-*a* Concentrations in Utah Lake
Using Landsat 7 ETM+ Imagery

Victor Nii Afum Narteh
Department of Civil & Environmental Engineering, BYU
Master of Science

This study shows the results of testing previous research that used remote sensing techniques to determine chlorophyll-*a* concentrations in turbid surface waters, and developing similar methods and models for Utah Lake using Landsat 7 ETM+ satellite imagery and field measured concentrations of chlorophyll-*a*. The data for the study included images acquired on June 22 and July 8, 2009. The field data included ground measurements taken on June 22 and July 6, 2009 from seven water quality sampling locations. The 48 hour time difference between the Landsat image acquisition (July 8) and the field measurement (July 6), and the small sample size for the data analysis were potential sources of error.

The log transformation of red/near-infrared reflectance (i.e. ln[Band3/Band4]) had a high correlation with the field measured chlorophyll-*a* concentrations (R^2 = 0.9337). With this relationship, a model and 19 contour maps showing the spatial distribution of chlorophyll-*a* concentrations over Utah Lake was developed for the spring, summer, and fall seasons of 2003 to 2010. Generally about 90% of the Lake area had chlorophyll-*a* concentrations lower than 20µg/L. High concentrations of Chlorophyll-*a* (355µg/L and over) were observed mostly at the Provo Bay and Goshen Bay areas of the Lake. Occasionally, elevated levels of chlorophyll-*a* were observed at the northeastern, middle, and western sections of the lake. Utah Lake's average chlorophyll-*a* concentration is declining over time. In spring, the Lake average chlorophyll-*a* concentration reduced from 30.51µg/L in 2004 to 7.08µg/L in 2010. In summer, this average reduced from 132.13µg/L in 2003 to 36.58µg/L in 2010. Finally, in fall, the Lake average chlorophyll-*a* concentration reduced from 273.40µg/L in 2006 to 33.59µg/L in 2010.

Field measured concentrations of phosphorus and model estimates for chlorophyll-*a* concentrations were highly correlated (R^2 = 0.9046). This suggests that the elevated levels of chlorophyll-*a* might be a result of the point and non-point discharge of phosphorus-laden wastewater from treatment plants, municipal storm drains, and agricultural activities.

.

Keywords: Victor Nii Afum Narteh, remote sensing, chlorophyll-*a*, landsat 7 ETM+

ACKNOWLEDGMENTS

I am grateful for the support of my advisor and committee chair, Dr. M. Brett Borup, who provided me with mentoring and also located grant opportunities that brought in funding for this work. Gratitude goes to the rest of my committee members, Dr. A. Woodruff Miller and Dr. Gustavious P. Williams, for their recommendations and support. Special thanks to Oliver Obregon, a PhD student at Brigham Young University who helped me with the analysis of water quality data. David Fayol, a graduate student at Brigham Young University, helped me understand the technicalities of the ENVI software. Water quality ground measurements for Utah Lake was provided by Kate Tipple of the Utah Division of Water Quality. Finally, I am grateful to my family and friends who contributed to the success of this work.

TABLE OF CONTENTS

LIST OF TABLES ..... **vii**

LIST OF FIGURES ..... **ix**

1 Introduction **1**

1.1 Problem Statement 2

1.2 Objectives 2

1.3 Utah Lake Overview 3

2 Literature Review **5**

2.1 Remote Sensing Overview 5

2.2 Previous Studies on Remote Sensing Measurements of Chlorophyll-*a* in Turbid Waters 7

3 Methods and Data **11**

3.1 Insitu and Laboratory Assays 11

3.2 Satellite Data 13

3.3 Atmospheric Correction 15

3.4 Locating Pixel Data 17

3.5 Chlorophyll-*a* Model Selection 18

3.6 Time Lag between Field Measurement and Landsat Data 21

3.7 Mapping Chlorophyll-*a* over Utah Lake 22

4 Analysis **23**

4.1 Contour Maps 23

4.2 Correlation and Trend 33

5 Discussion **35**

6 Conclusion **39**

REFERENCES **41**

Appendix A. Other Band Reflectance Models 43

Appendix B. Landsat Calibration 49

LIST OF TABLES

Table 3-1: Sample sites for chlorophyll-*a* measurements in Utah Lake 11

Table 3-2: June 22, 2009 field data for chlorophyll-*a* concentrations 13

Table 3-3: July 06, 2009 field data for chlorophyll-*a* concentrations 13

Table 3-4: Spectral and spatial resolutions for Landsat 7 ETM+ Satellite 14

Table 3-5: Wind data from Provo Municipal Airport station from July 6 to July 8, 2009 21

LIST OF FIGURES

Figure 2-1: Reflectance characteristics for clear water and algae-laden water 9

Figure 3-1: Seven Utah Lake water sample sites.....12

Figure 3-2: A schematic of the sun-sensor pathway.....15

Figure 3-3: ENVI Landsat calibration parameters.....16

Figure 3-4: Using the pixel locator tool to locate pixels for STORET 4917500.....17

Figure 3-5: Spectral profile for STORET 4917500.....18

Figure 3-6: Field measured chlorophyll-a vs. ln[Band 3/Band 4].....19

Figure 3-7: Distribution of pixel data points.....22

Figure 4-1: Chlorophyll-a mapping over Utah Lake for spring 2004.....23

Figure 4-2: Chlorophyll-a mapping over Utah Lake for spring 2005.....24

Figure 4-3: Chlorophyll-a mapping over Utah Lake for spring 2006.....24

Figure 4-4: Chlorophyll-a mapping over Utah Lake for spring 2007.....25

Figure 4-5: Chlorophyll-*a* mapping over Utah Lake for spring 2008.....25

Figure 4-6: Chlorophyll-*a* mapping over Utah Lake for spring 2009.....26

Figure 4-7: Chlorophyll-*a* mapping over Utah Lake for spring 2010.....26

Figure 4-8: Chlorophyll-*a* mapping over Utah Lake for summer 2003.....27

Figure 4-9: Chlorophyll-*a* mapping over Utah Lake for summer 2004.....27

Figure 4-10: Chlorophyll-*a* mapping over Utah Lake for summer 2005.....28

Figure 4-11: Chlorophyll-*a* mapping over Utah Lake for summer 2006.....28

Figure 4-12: Chlorophyll-*a* mapping over Utah Lake for summer 2007.....29

Figure 4-13: Chlorophyll-*a* mapping over Utah Lake for summer 2008.....29

Figure 4-14: Chlorophyll-*a* mapping over Utah Lake for summer 2009.....30

Figure 4-15: Chlorophyll-*a* mapping over Utah Lake for summer 2010.....30

Figure 4-16: Chlorophyll-*a* mapping over Utah Lake for fall 2006 31

Figure 4-17: Chlorophyll-*a* mapping over Utah Lake for fall 2007 31

Figure 4-18: Chlorophyll-*a* mapping over Utah Lake for fall 2009 32

Figure 4-19: Chlorophyll-*a* mapping over Utah Lake for fall 2010 32

Figure 4-20: Correlation between concentrations of total phosphorus (field) and chlorophyll-*a* (model) 33

Figure 4-21: Average chlorophyll-*a* concentration for Utah Lake 34

Figure 5-1: Wastewater treatment plants and other sources of wastewater discharge into Utah Lake 36

Figure A-1: Field measured chlorophyll-*a* vs. Band 3/Band 4 (power trendline) 43

Figure A-2: Field measured chlorophyll-*a* vs. Band 3/Band 4 (logarithmic trendline)..... 44

Figure A-3: Field measured chlorophyll-*a* vs. Band 3/Band 4 (linear trendline) 44

Figure A-4: Field measured chlorophyll-*a* vs. Band 3/Band 4 (polynomial trendline)..... 45

Figure A-5: Field measured chlorophyll-*a* vs. Band 4/Band 3 (linear trendline) 45

Figure A-6: ln chlorophyll-*a* vs. ln[Band 3/Band 4] (power trendline)..... 46

Figure A-7: ln chlorophyll-*a* vs. ln[Band 3/Band 4] (polynomial trendline) 46

Figure A-8: Field measured chlorophyll-*a* vs. (Band 1 – Band 3)/Band 2 (polynomial trendline) 47

Figure A-9: ln[chlorophyll-*a*] vs. (Band 1 – Band 3)/Band 2 (polynomial trendline) 47

Figure A-10: ln chlorophyll-*a* vs. ln (Band 1 – Band 3)/Band 2 (polynomial trendline) 48

1 INTRODUCTION

The quality of a water body is described by its physical, chemical, thermal and/or biological characteristics. Water quality is affected by materials from point sources and/or non-point sources. Point sources can be traced to a single source, like a pipe or drain. Non-point sources are diffuse and respond to the nature of the landscape, water movement, land use, soil type, and/or other anthropogenic activities. Anthropogenic activities like agriculture, industrialization, and rapid urbanization contribute polluting substances that lead to the deterioration of the water quality of most freshwater and estuarine ecosystems in the world .

In the United States, off-site downstream deterioration of water quality has been estimated to cost billions of dollars each year . As a result, monitoring and assessing the quality of surface waters periodically are critical.

The purpose of this study is to develop empirical/analytical models to express chlorophyll-*a* concentrations using remote sensing techniques for monitoring and assessing water quality in Utah Lake.

Recent studies on Utah Lake by the Utah Division of Water Quality (UDWQ) show that the phosphorus levels in the lake is very high and that 76% of the phosphorus content comes from discharges from surrounding wastewater treatment facilities that discharge effluents directly or indirectly into the lake.

Phosphorus in lakes is a limiting nutrient essential to aquatic life and in nature exists as part of the phosphate ions. High phosphates levels contribute to pollutions in water bodies and the Utah Lake is no exception. This enrichment caused by excess phosphates promotes algae blooms. In addition to odor and aesthetic problems, high algae growth reduces the amount of dissolved oxygen in the lake because as algae grow and die, more oxygen in the lake is consumed in the process. This reduction of dissolved oxygen affects the lake's ecosystem negatively and as a result many fish die.

Previous researches have shown that there is a good correlation between total phosphorus and chlorophyll-*a*. With knowledge of the chlorophyll-*a* concentration in Utah Lake, a good estimate of the impact of the discharge from neighboring wastewater treatment plants on the phosphorus levels in Utah Lake can be made.

1.1 Problem Statement

Although field measurements taken at monitoring stations can be used to track temporal changes in chlorophyll-*a* concentrations for that particular point, they cannot be used to detail changes across the entire stretch of water surface. To avoid missing important details, there is a need to account for spatial variations over the entire lake using procedures that use the relatively cheap and readily available Landsat Enhanced Thematic Mapper plus (ETM+) satellite imagery data.

1.2 Objectives

1. Based on previous research that used remote sensing techniques to determine chlorophyll-*a* concentration in surface waters, develop similar methods and models for

Utah Lake using Landsat 7 ETM+ satellite imagery and field measured concentrations of chlorophyll-*a*.

2. If the model results show good correlation with observed data, map the chlorophyll-*a* concentrations for Utah Lake in the spring, summer, and fall seasons of 2003 to 2010.
3. Develop a correlation between model estimates for chlorophyll-*a* concentrations and field measured phosphorus concentrations.
4. Make observations about correlation between chlorophyll-*a* concentration and known wastewater discharge points.

1.3 Utah Lake Overview

Utah Lake is located in north-central Utah near the cities of Orem and Provo. It is the largest freshwater lake in the state, as well as the largest naturally occurring freshwater lake in the western United States. Utah Lake is listed as a 2B, 3B, 3D, 4 lake. The beneficial uses of Utah Lake as designated by the State of Utah (Utah Administrative Code R317-2-13-12, June 01, 2006) include: secondary contact recreation (activities like boating, wading, etc); warm water game fish and associated food chain; waterfowl, shore birds and other water-oriented wildlife and associated food chains; and agricultural water supply . The lake is 24 miles long and 13 miles wide, at its greatest, with a surface area of approximately 96,600 acres and a volume of 902,400 ac-ft. The relatively small volume of the lake is due to its shallow depth. The lake has a maximum depth of about 18 feet and the average depth is about 10 feet .

Primary inflows to the lake are from the American Fork River, the Provo River, Mill Race Creek, Hobble Creek, the Spanish Fork River, and Currant River. The Provo River is the major contributor to Utah Lake's inflow. The lake's major outlet is the Jordan River (located at the north end of the lake) that flows into the Great Salt Lake .

Utah Lake is a highly productive lake that experiences extensive algal blooms in the late summer and fall. The lake is listed on Utah's 2004 § 303(d) list for exceedance of state criteria for total phosphorus. Utah Lake is often considered to be a hyper-eutrophic ecosystem, with the highest algal diversity in spring and early summer, decreasing with the progression of the seasons.

Utah Lake is a large, shallow, semi-terminal water body that is fed by a very large, mostly Mesozoic-aged nutrient-rich sediment basin . Phosphorus, the nutrient that limits the growth of algae in surface waters, has a tendency to sorb onto these suspended sediments and settle at the bottom of the lake. Because of the lake's shallow depth, wind action constantly stir up and mix bottom sediments. This condition causes phosphorus to be released from sediments in the benthic zone. The released phosphorus mixes with the oxygenated water at the epilimnion resulting in algae blooms. Other concerns associated with elevated total phosphorus concentrations include periphyton growth, low dissolved oxygen, increased pH, and cyanotin production by blue-green algae (cyanobacteria).

2 LITERATURE REVIEW

2.1 Remote Sensing Overview

One of the major factors affecting water quality in water bodies across the landscape is algae which can be measured by estimating chlorophyll. Monitoring the concentrations of chlorophyll is necessary for managing eutrophication in lakes . Several methods for chlorophyll analysis are available and these methods are described in the Standard Methods . Conventional chlorophyll-*a* concentration measurement involves grab sampling followed by laboratory assay that require considerable amount of time, effort, and resources.

Remote sensing tools provide spatial and temporal views of surface water quality parameters that are not readily available from in situ measurements. This makes it possible to monitor the landscape effectively and efficiently by identifying and quantifying water quality parameters and problems. Algae change the energy spectra of reflected solar and/or emitting thermal radiation from surface waters which can be measured using remote sensing techniques .

Remote sensing techniques for monitoring water quality began in the early 1970s. These early methods measured spectral and thermal differences in emitted energy from water surfaces. The presence of substances in surface water can significantly change the backscattering characteristics of surface water . Remote sensing techniques measure these changes in the solar radiation reflected from the water surface and relate these measured changes to a water quality parameter using empirical/analytical models.

Most remote sensing studies of chlorophyll in water are based on empirical relationships between radiance/reflectance in narrow bands or band ratios, and chlorophyll. Field measurements are compared with empirical models for calibration purposes. A model is calibrated when the model output matches field data; this is achieved by adjusting or modifying the input parameters in the model's algorithm.

The following algorithm based on aircraft measurements to determine seasonal patterns of chlorophyll in the Chesapeake Bay was developed:

$$\log_{10}[\text{Chlorophyll}] = a + b(-\log_{10}G) \quad (2\text{-}1)$$

where a and b are empirical constants derived from in situ measurements and G is $(R_2)^2/(R_1 \times R_3)$]. R_1, R_2, and R_3 are radiance at 460nm, 490nm, and 520nm respectively.

NASA's Moderate Resolution Imaging Spectroradiometer (MODIS) remote sense data was used to develop chlorophyll-*a* concentration monitoring support models in Chesapeake Bay. These models include ambient water temperature as a contributing independent variable. The model developed for March is shown in equation 2-2 below:

$$\ln(\text{chlo.a}) = [-0.6157 \times \text{Temp}] + [3.4175 \times \ln(\text{Temp})] + [0.0725 \times \ln(B1/B2)] \quad (2\text{-}2)$$

where chlo.a represents chlorophyll (mg/L); Temp represents ambient temperature (˚C); B1 represents MODIS surface reflectance in the red band; B2 represents MODIS surface reflectance in the near-infrared (NIR) band.

2.2 Previous Studies on Remote Sensing Measurements of Chlorophyll-*a* in Turbid Waters

There have been relatively successful attempts in the United States to use Landsat Thematic Mapper imagery to determine chlorophyll-*a* concentrations in large open surface waterbodies. One of such studies involved the combination of Landsat Thematic Mapper (TM) satellite images and field measurements to model and map spatial distributions of chlorophyll-*a* in the Lake Manassas Reservoir. A ratio of Landsat TM band 3 and Landsat Band 4 was used in a regression with data collected at eight water quality monitoring stations run by the Occoquan Watershed Monitoring Lab. Correlation coefficients of 0.76 for the 1998 data and 0.73 for the 2000 data were achieved. Cross validation statistical analysis was used to check the accuracy of the two models . The methodology employed in this research could be criticized because the ground measurements were taken 24 hours prior to the acquisition of satellite image data, the small sample size of the chlorophyll-*a* measurements, and uncertainty in the locations of monitoring stations.

Although remote sensing methods can estimate chlorophyll, it has some limitations. Studies have shown that the broad wavelength of spectral data available on old satellites like Landsat and SPOT, do not permit discrimination of chlorophyll in waters with high suspended sediments . This is a result of the dominance of the spectral signal from the suspended sediments.

However, research has shown that even in the presence of high suspended sediment concentrations that can dominate the spectrum, the linear relationship between chlorophyll and the narrow band spectral details at the “red edge” of the visible spectrum still exists

In an experiment to test the use of the well-documented ratio of near-infrared (NIR; 705 nm) to red (670 nm) reflectance in estimating chlorophyll content in Branched Oak Lake (a relatively turbid Midwestern reservoir), it was realized that with the exception of one occasion,

the NIR/red ratio was not a good predictor of algae-chlorophyll concentration . They concluded that in general, the first derivatives of reflectance (near 690 nm) gave a better correlation with chlorophyll. In another study by Han et.al, the commonly used NIR/red ratio was observed to be more suitable for chlorophyll-*a* concentrations less than 300 μg/L. The first derivative of reflectance of about 690nm was best suited for higher chlorophyll-*a* concentrations.

In an analysis of the spectral curves collected from two of the Loosdrecht Lakes in the Netherlands, it was found that the estimates of optical water quality (algae-chlorophyll inclusive) were made by using ratios of wavelengths between 600 nm and 720 nm .

Spectral interactions occur between suspended sediments and algal chlorophyll (Han et al. 1994). A study was carried out to characterize and compare the relationship between suspended sediment concentration and reflectance in clear and algae-laden waters. The research was based on a controlled experiment conducted outdoors using a large tank and natural sunlight. Two experiments were done—one was based on a background of clear well water and the other, a background of algae-laden water. By applying different amounts of red loam soil to the clear water and algae-laden water respectively, the concentration of suspended sediments in each case was varied. The sediments were kept in suspension by a mechanical pump-driven device. The stirring device operated continuously throughout the experiment .

As seen in figure 2-1, the algae-laden water without sediments reflectance curve peaks twice—the maximum reflectance occurs at the 550 nm wavelength while the second peak occurs at the 700 nm wavelength.

The analysis of dry sediments show increases in reflectance between 500 nm and 900 nm. When the soil is wet, this reflectance curve is dampened, due to the absorption of light by the water; however, the shape of the reflectance signature is maintained.

The same concentration of suspended sediments produced higher reflectance values between 400 nm and 700 nm in clear water than in algae-laden water due to the red and blue absorption of chlorophyll. At wavelengths between 700 nm and 900 nm, algae had little effect on the suspended sediment concentration reflectance relationship. It is important to note that at the near-infrared (NIR) spectrum (700 nm), the reflectance increases linearly with increasing suspended sediment concentration.

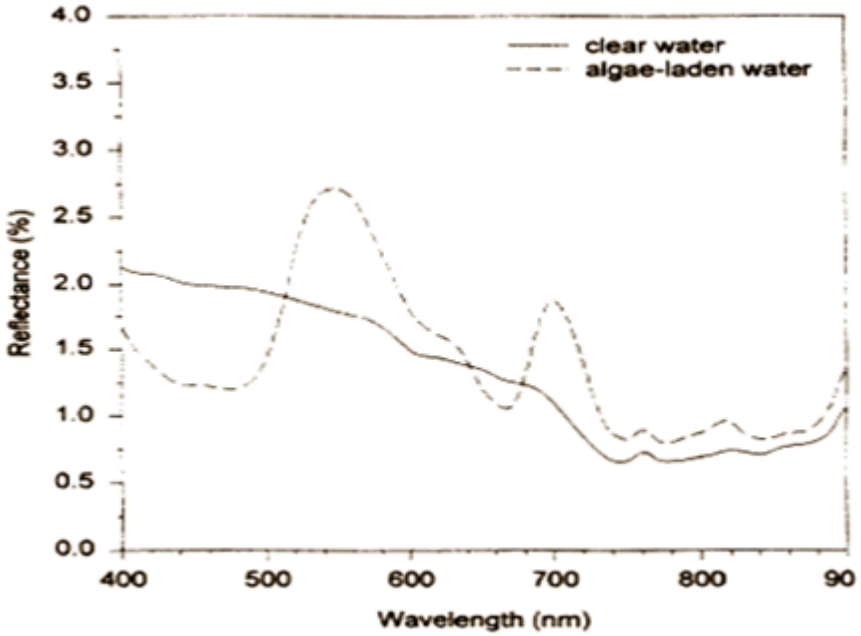

Figure 2-1: Reflectance characteristics for clear water and algae-laden water

Dr. Han's experiment shows that it is feasible to use remote sensing techniques to determine the concentration of suspended sediment and algae in large water bodies. Mittenzewy et al., using hyperspectral data, found a high coefficient of determination (0.98) using the NIR/red reflectance ratio , but Han et al., found that the uncertainty for this ratio grows as the chlorophyll-*a* concentration dips below 10 μg/L. Another method is to use a NIR-red difference,

although this method seems to work only for waters with little or no sediment (Han, et al., 1997). The NIR-red difference is suggested as a means of compensating the effects of increased reflectance in algae-laden waters with sediment particles, for wavelengths longer than 550 nm.

3 METHODS AND DATA

3.1 Insitu and Laboratory Assays

Chlorophyll-*a* insitu and laboratory measurements were sourced from the Utah Division of Water Quality for the period of study (January 2008 to Dec 2010). Field data were acquired for June 22, 2009 and July 06, 2009. These measured data was used to calibrate and validate the models developed from the remote sensing methods. The seven sample sites in Utah Like are illustrated in Table 3-1 and Figure 3-1 below.

Table 3-1: Sample sites for chlorophyll-*a* measurements in Utah Lake

STORET	Site Description	Latitude	Longitude
4917310	UTAH LAKE 0.5 MILE WEST OF GENEVA DISCHARGE #15-A	40.320917	-111.776778
4917370	UTAH LAKE 1 MILE EAST OF PELICAN POINT	40.268333	-111.829167
4917450	UTAH LAKE AT MIDDLE OF PROVO BAY	40.189183	-111.699172
4917500	UTAH LAKE 3 MILE WEST-NORTHWEST OF LINCOLN BEACH	40.169722	-111.870833
4917520	UTAH LAKE 2 MILE OF SARATOGA SPRINGS #12	40.342222	-111.870556
4917600	UTAH LAKE GOSHEN BAY SOUTHWEST END	40.060278	-111.873611
4917770	UTAH LAKE OUTSIDE ENTRANCE TO PROVO BAY	40.188611	-111.730556

Figure 3-1: Seven Utah Lake water sample sites

The chlorophyll-*a* data measured from the above sample sites for both June 22, 2009 and July 06, 2009 datasets are shown in table 3-2 and table 3-3. The ranges of the data are small in terms of the change that would occur in the reflective response that might be perceived by a Landsat Thematic Mapper satellite sensor. These small values might be troublesome in the model calibration process.

Table 3-2: June 22, 2009 field data for chlorophyll-*a* concentrations

STORET ID	Chlorophyll-*a* (μg/L)
4917310	11.1
4917370	5.2
4917450	45
4917500	6.3
4917520	8.6
4917600	15.4
4917770	5

Table 3-3: July 06, 2009 field data for chlorophyll-*a* concentrations

STORET ID	Chlorophyll-*a* (μg/L)
4917310	13.1
4917370	10.9
4917450	113.4
4917500	8.9
4917520	7
4917600	17.5
4917770	14.8

From literature, previous remote sensing studies of chlorophyll-*a* data were less reliable when field concentrations were less than 10 μg/L. About 50% of the field data for June 22 fall below 10 μg/L. These low values might pose a problem in the calibration stage.

3.2 Satellite Data

The Landsat acquisition dates for the data used in this study are June 22, 2009 and July 08, 2009. Images with minimum cloud cover were sourced from the United States Geologic Service (USGS). The image for June 22 had about 19% cloud cover, while that of July 08 had 0% cloud cover.

These images were taken with the latest satellite from the Landsat program (Landsat7, launched on April 15, 1999). The distribution of the chlorophyll was estimated and mapped over Utah Lake using Landsat Enhanced Thematic Mapper Plus (Landsat ETM+). Landsat ETM+ has been widely used for water quality analysis because of its wide spatial resolution and suitable spectral range of data acquisition. Each band is useful for capturing different land cover aspects as shown in table 3-4 below.

Table 3-4: Spectral and spatial resolutions for Landsat 7 ETM+ Satellite

BAND	SPECTRAL RESOLUTION (nm)	SPATIAL RESOLUTION	MAPPING USES
Band 1: Blue	450 - 515	30 m × 30 m	Bathymetric mapping, distinguishing soil from vegetation and deciduous from coniferous vegetation
Band 2: Green	525 – 605	30 m × 30 m	Emphasizes peak vegetation, which is useful for assessing plant vigor
Band 3: Red	630 - 690	30 m × 30 m	Discriminates vegetation slopes
Band 4: Near-infrared	760 - 900	30 m × 30 m	Emphasizes biomass content and shoreline
Band 5: Mid-infrared	1550 - 1750	30 m × 30 m	Discriminates moisture content of soil and vegetation; penetrates thin clouds
Band 6: Thermal	10400 - 12500	60 m × 60 m	Thermal mapping and estimated soil moisture
Band 7: Far-infrared	2080 - 2350	30 m × 30 m	Hydrothermally altered rocks associated with mineral deposits
Band 8: Panchromatic	520 - 920	15 m × 15 m	Meter resolution, sharper image definition

Landsat 7 ETM+ images come with visible black streaks because of Scan Line Correction (SLC) failure. These black streaks are gaps in the pixel data and could be possible source of

errors because of missing data. Landsat 7 ETM+ is still capable of acquiring useful images because these gaps are more pronounced at the edge of the scene and gradually diminish toward the center. The U.S. Geological Survey (USGS) Earth Resources Observation Systems (EROS) Data Center (EDC) has developed multi-scene (same path/row) gap-filled products to improve the usability of ETM+ data acquired after May 31, 2003 SLC failure.

Most Landsat scenes (like those used in this study) are processed as Level 1T (precision and terrain corrected); however, certain scenes do not have ground-control or elevation data necessary for precision or terrain correction. In these cases the best level of correction is applied (Level 1G-systematic or Level 1Gt-systematic terrain).

3.3 Atmospheric Correction

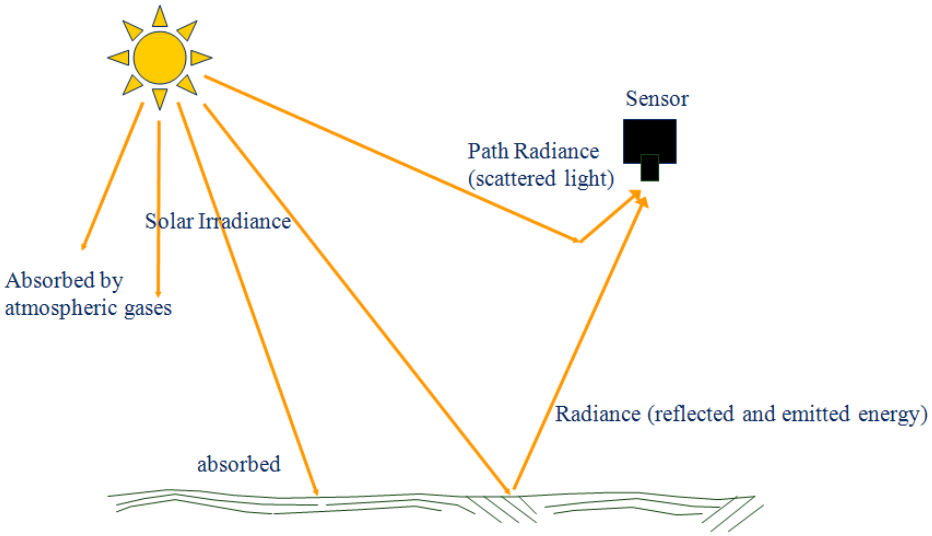

Figure 3-2: A schematic of the sun-sensor pathway

As shown in figure 3-2, data acquired from remote sensing requires that solar radiation pass through the atmosphere before it is collected by the sensors. As a result, raw remote sensing

data include errors from factors such as: noise, aerosols, water vapor, surface reflectance, solar irradiance curve, atmospheric effects (scattering and absorption), variation in illumination due to topography, and instrument response. To allow for proper quantitative analysis, the errors introduced by these factors need to be eliminated so that raw data from the images can be converted to reflectance. This process is called atmospheric corrections. Atmospheric correction was performed using Dark Subtraction—a method that subtracts the dark noise from the image. Prior to the correction, the Landsat Calibration option in ENVI version 4.7 was used to convert Landsat ETM+ digital numbers to exoatmospheric reflectance (reflectance above the atmosphere) using published post-launch gains and offsets found in the Landsat imagery metadata file. The dialogue boxes in Figure 3-3 show the parameters for Landsat calibration in ENVI.

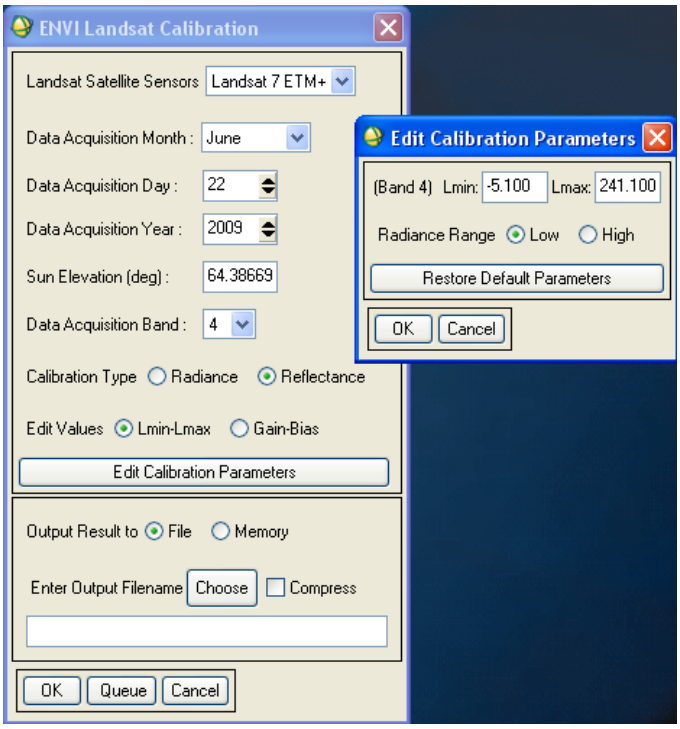

Figure 3-3: ENVI Landsat calibration parameters

When the metadata file is available, ENVI automatically populates the calibration parameter fields. Otherwise, ENVI inputs default values in the calibration parameter fields.

3.4 Locating Pixel Data

In order to extract reflectance data that correspond to the individual sample site locations on the Landsat imagery, the pixel locator tool in ENVI 4.7 was used. This was the most preferred option because Landsat ETM+ images contain georeferenced data, thereby providing an easier, faster, and more accurate method for locating the sampling sites. As illustrated in Figure 3-4 below, in the pixel locator dialogue box, the user can locate pixels by specifying map/geographic coordinates. When the desired coordinates has been entered, the zoom box jumps to the specified pixel location. The pixel locator has the option to offset the image location to the nearest pixel when it cannot find a pixel for the specified coordinate.

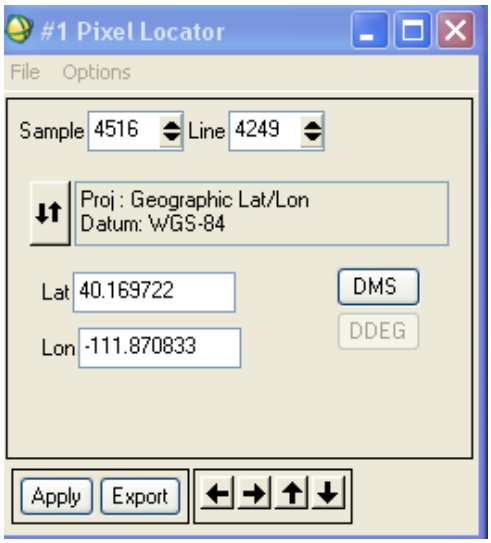

Figure 3-4: Using the pixel locator tool to locate pixels for STORET 4917500

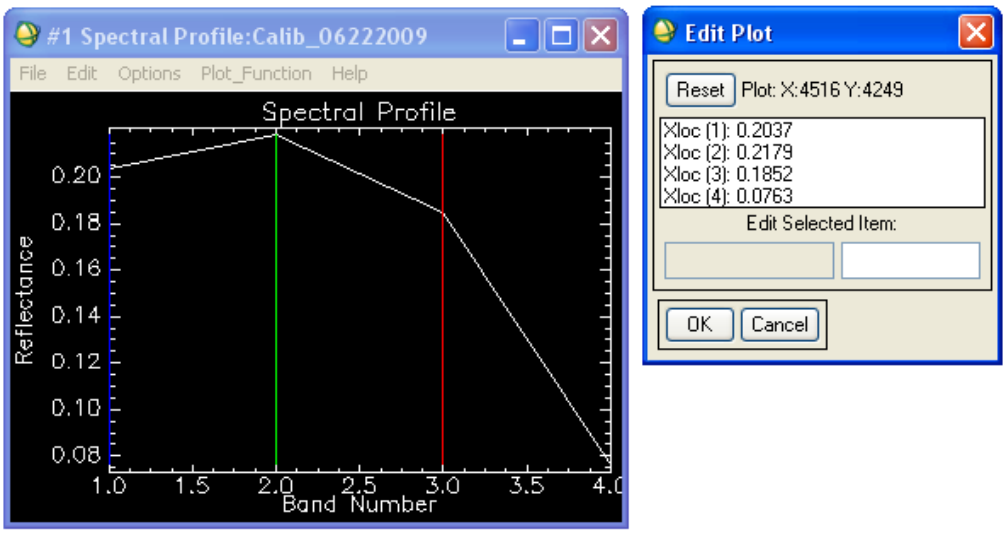

Figure 3-5: Spectral profile for STORET 4917500

Figure 3-5 shows the pixel location spectral profile for STORET 4917500. This is a plot of reflectance vs. band number. From Figure 3-5 it can be seen that the only bands imported into ENVI were band 1 (blue band), band 2 (green band), band 3 (red band), and band 4(near-infra red). This is because previous researchers developed relationships between chlorophyll-*a* concentrations and the first four bands i.e. blue, green, red, and near-infra red bands . This study is also focusing on only these particular bands as well.

3.5 Chlorophyll-*a* Model Selection

Several band reflectance relationships have been suggested in many literatures related to determining chlorophyll-*a* concentrations using remote sensing methods. In order to determine which of the suggested band reflectance ratios, relationships, and transformations will yield the best correlation with chlorophyll-*a* field data, several scatter plots were made. A total of 14 datasets were used for the initial model analysis. The data for these initial plots comprised of the

entire field measured data (June 22 and July 6, 2009) and band reflectance data (June 22 and July 8, 2009) for all seven sampling sites.

There was a poor correlation between (Band 1 – Band 3)/Band 2 reflectance ratios and field measured chlorophyll-*a* (See Appendix A). The relationship between field measured chlorophyll-*a* concentrations and the log transformation of (Band 3/Band 4) reflectance ratio had the best model that fit the physical process. The empirical relationship for the chlorophyll-*a* model was derived from the polynomial regression curve (See Figure 3-6). Due to the high R^2 value of 0.9335 and the small datasets, outlier detection and removal were ignored.

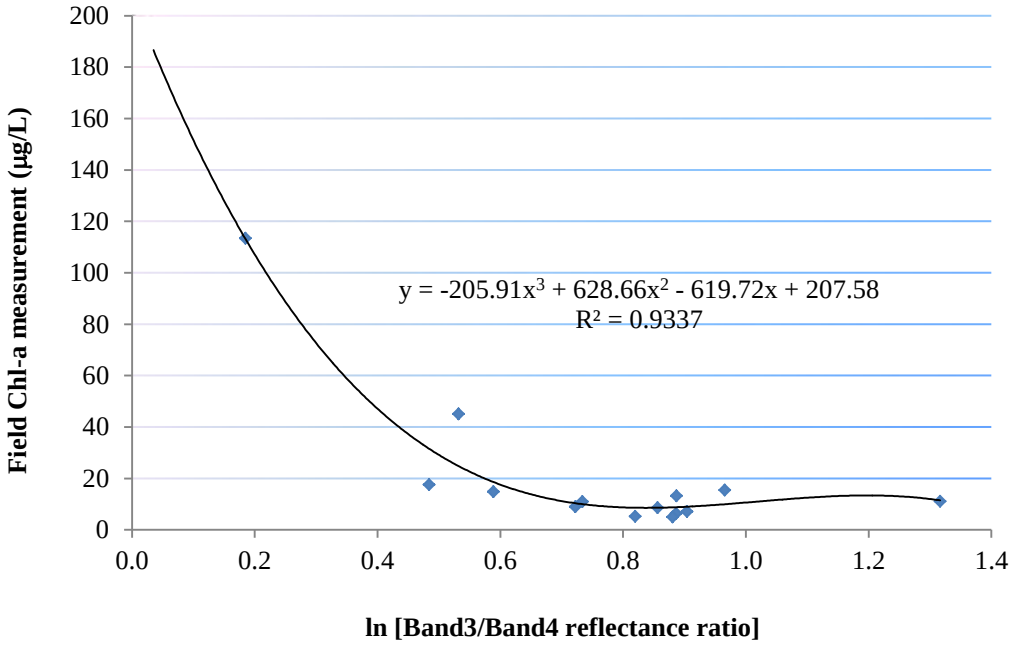

Figure 3-6: Field measured chlorophyll-*a* vs. ln[Band 3/Band 4]

This model equation (see equation 3-1) would be used in the remainder of this research to estimate and map concentrations of chlorophyll-*a* in Utah Lake for the spring, summer, and fall seasons from 2003 to 2010.

Chlorophyll-*a* = $-205.91x^3 + 628.66x^2 - 619.72x + 207.58$ (3-1)

where x = ln (Band 3/Band 4) reflectance ratio, and the estimated chlorophyll-*a* concentration is in μg/L.

The following steps are guidelines for acquiring, processing, and using the chlorophyll-*a* model to produce chlorophyll-*a* spatial and temporal maps:

1. Acquire Landsat Images from the USGS Globalization Viewer or USGS Earth Explorer.
2. In ENVI, use the Landsat Calibration tool to convert Image digital numbers (DN) to exoatmospheric reflectance data.
3. In ENVI, use the Dark Subtract tool to remove noise from the image. Perform other atmospheric corrections if possible.
4. Use ENVI's band math or band ratio image processing tool to automate pixel computations.
5. Create Regions of Interest (ROI) and use that to export pixel values to ASCII file.
6. Convert ASCII file to a file format readable in ArcGIS. (File should contain X,Y location data)
7. Import table into ArcGIS, Display XY Data, and export data to a feature class.
8. Perform interpolation in ArcGIS to create colored contour map.

The following are hints to consider when using the model for estimation of chlorophyll-*a* concentrations at sampling sites:

1. If an estimation for chlorophyll-*a* concentration yields a negative value, consider the nearest neighboring pixels for new band reflectance ratios.
2. If the new ratios from step 1 still yield negative values, then the estimated chlorophyll-*a* concentration for that sampling point is 0.

3.6 Time Lag between Field Measurement and Landsat Data

Most likely, the major source of error lies with the 48 hour time difference between chlorophyll-*a* field measured date (July 6, 2009) and the Landsat image acquisition date (July 8, 2009). During this time, the algae in the lake could have been displaced by winds that mix the epilimnion or some aquatic recreational activities. Table 3-5 is a summary of wind data from the National Oceanic and Atmospheric Administration (NOAA) Provo Municipal Airport station recorded from July 6 to July 8, 2009.

Table 3-5: Wind data from Provo Municipal Airport station from July 6 to July 8, 2009

Date	Wind Speed	Wind Type	Direction Angle
July 6, 2009	2.6 miles/hr	Normal	between 20° and 220°
July 7, 2009	2.7 miles/hr	Normal	between 20° and 360°
July 8, 2009	4.5 miles/hr	Normal	between 30° and 340°

The direction angle in table 3-5 is the angle measured in a clockwise direction between true north and the direction from which the wind is blowing. The velocity of wind driven surface water currents (depth < 1.0 cm) is approximately 0.02 times the wind speed. This relationship is linear up till a wind speed of about 6 meters per second or a little more than 13 miles per hour . Theoretically, a wind blowing at a speed of 2.6 miles per hour over the surface of Utah Lake can displace the water surface to a distance of 2.5 miles in two days.

Other agents of water dispersion include: water density differentials caused by radiant energy, recreational activities (such as boating, wading, etc), and the Coriolis effect (deflection of moving objects caused by the Earth's rotation and the inertia of the mass experiencing the effect).

3.7 Mapping Chlorophyll-*a* over Utah Lake

The estimated concentration of chlorophyll-*a* was distributed over Utah Lake using the Inverse Distance Weighted (IDW) interpolation tool in ArcMap version 10. The interpolation was based on the estimated chlorophyll-*a* concentrations for 370 pixel data points. A mask was included in the analysis to limit the interpolation to the confines of Utah Lake.

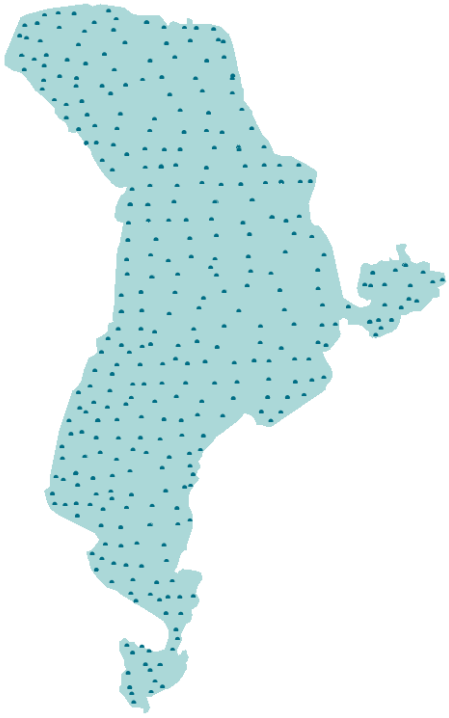

Figure 3-7: Distribution of pixel data points

4 ANALYSIS

4.1 Contour Maps

Figure 4-1 to figure 4-19 are contour maps that illustrate 19 seasonal distributions of chlorophyll-*a* concentration over Utah Lake from 2003 to 2010. The Total Maximum Daily Loading (TMDL) report for 2007, shows that the maximum chlorophyll-*a* concentration measured in Utah Lake was 354.6µg/L . Since it has not been proven whether the high extrapolated results from the model are reasonable, the maximum value of 355µg/L as shown in the map legend represents model estimates of chlorophyll-*a* that are 355µg/L and higher.

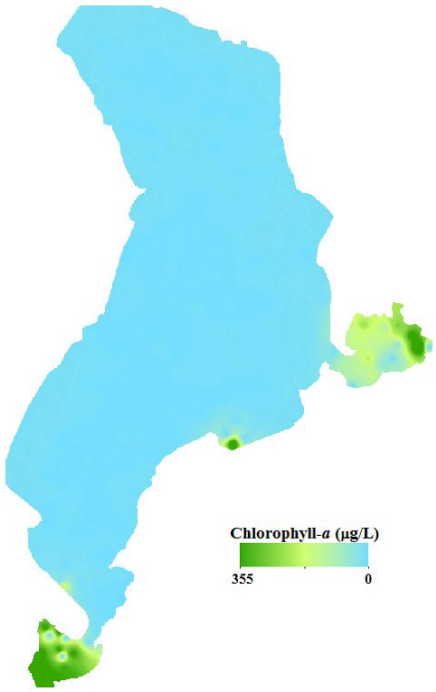

Figure 4-1: Chlorophyll-*a* mapping over Utah Lake for spring 2004

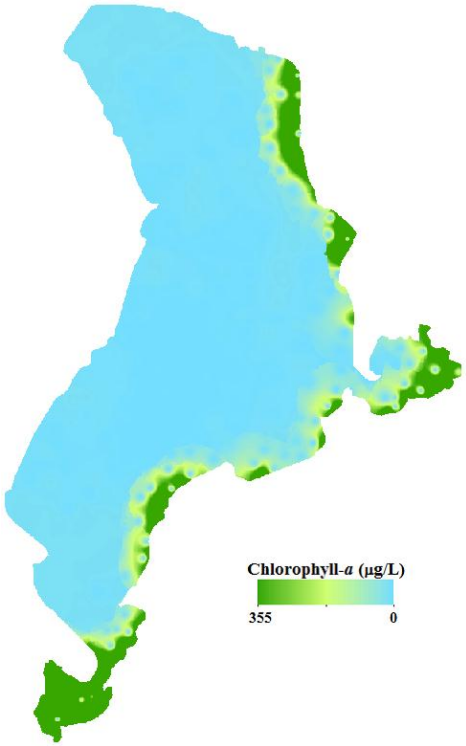

Figure 4-2: Chlorophyll-*a* mapping over Utah Lake for spring 2005

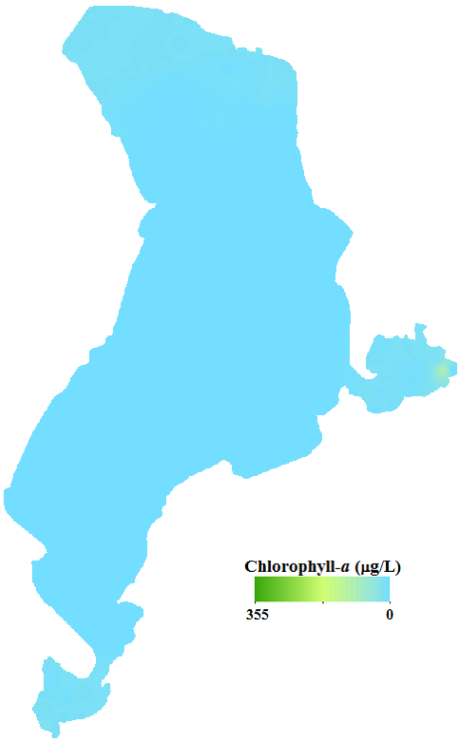

Figure 4-3: Chlorophyll-*a* mapping over Utah Lake for spring 2006

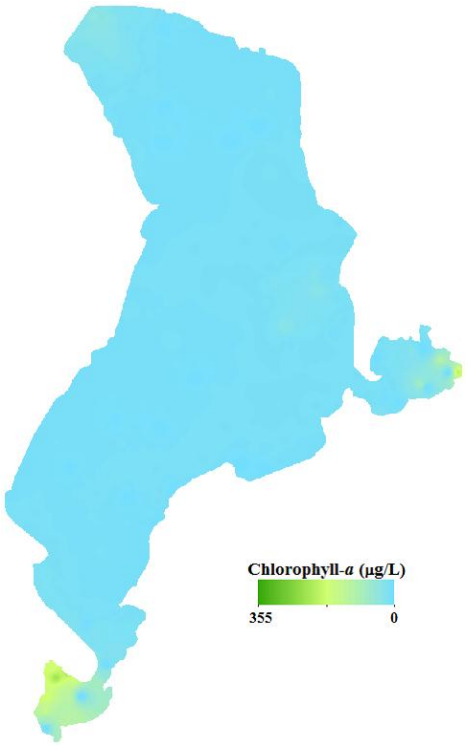

Figure 4-4: Chlorophyll-*a* mapping over Utah Lake for spring 2007

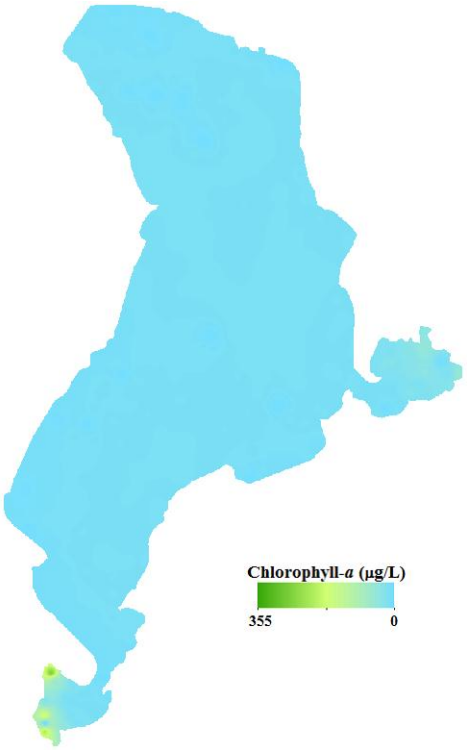

Figure 4-5: Chlorophyll-*a* mapping over Utah Lake for spring 2008

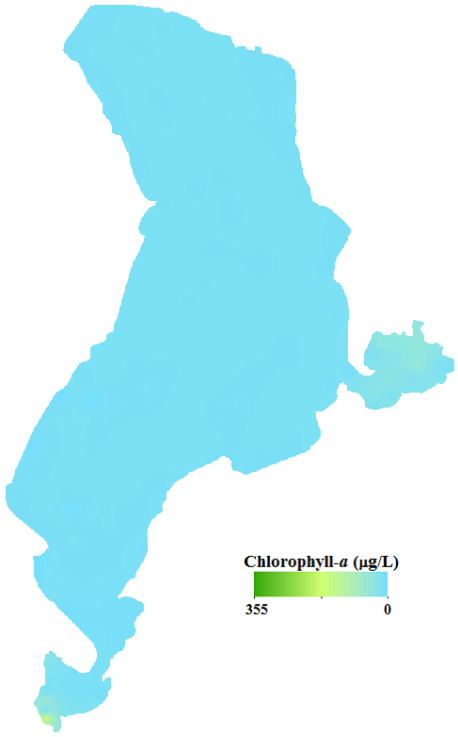

Figure 4-6: Chlorophyll-*a* mapping over Utah Lake for spring 2009

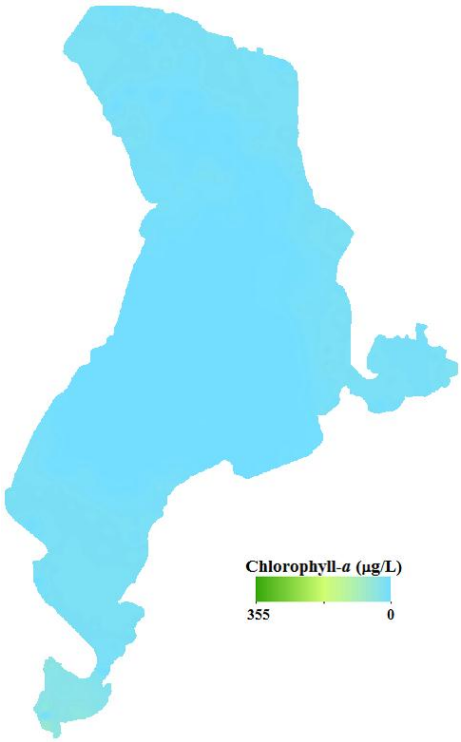

Figure 4-7: Chlorophyll-*a* mapping over Utah Lake for spring 2010

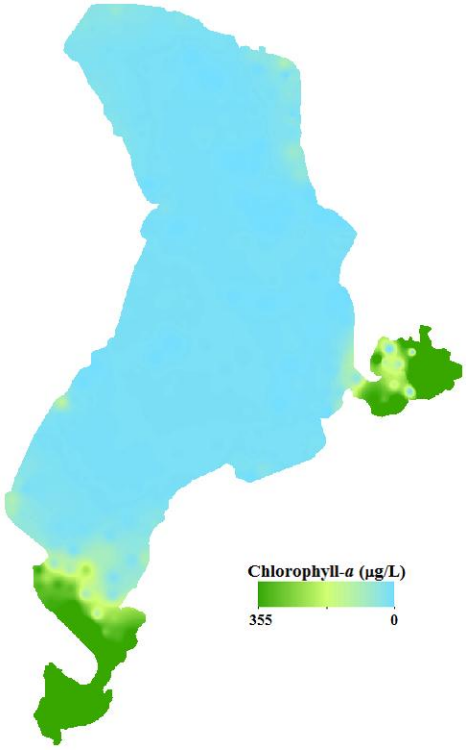

Figure 4-8: Chlorophyll-*a* mapping over Utah Lake for summer 2003

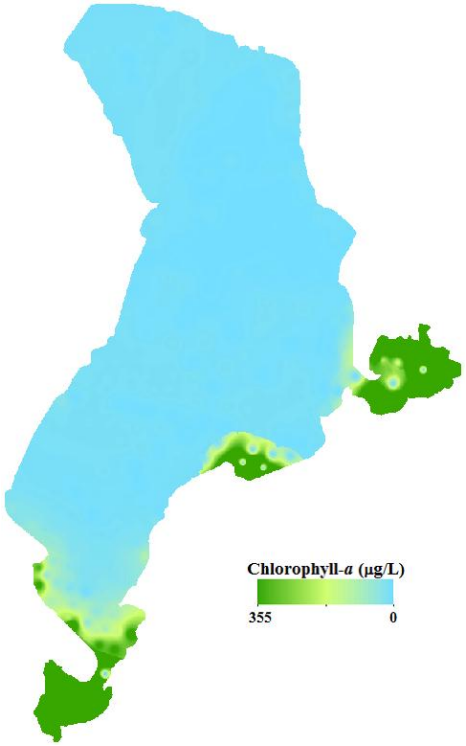

Figure 4-9: Chlorophyll-*a* mapping over Utah Lake for summer 2004

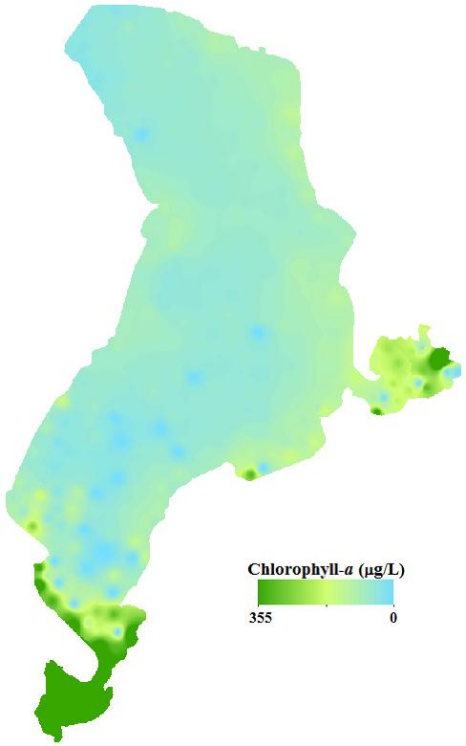

Figure 4-10: Chlorophyll-*a* mapping over Utah Lake for summer 2005

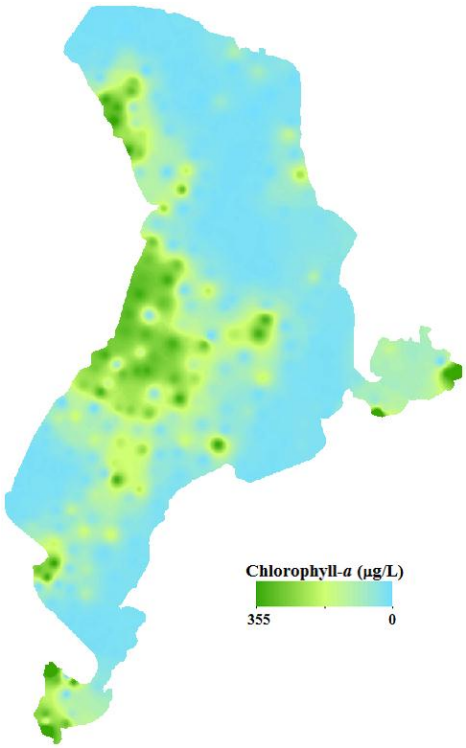

Figure 4-11: Chlorophyll-*a* mapping over Utah Lake for summer 2006

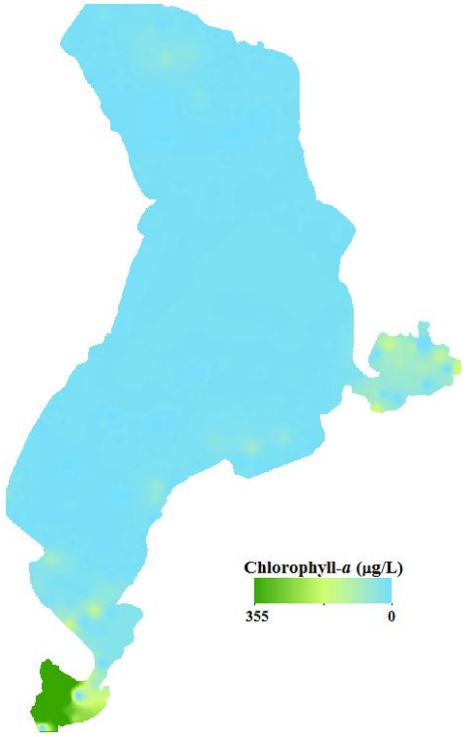

Figure 4-12: Chlorophyll-*a* mapping over Utah Lake for summer 2007

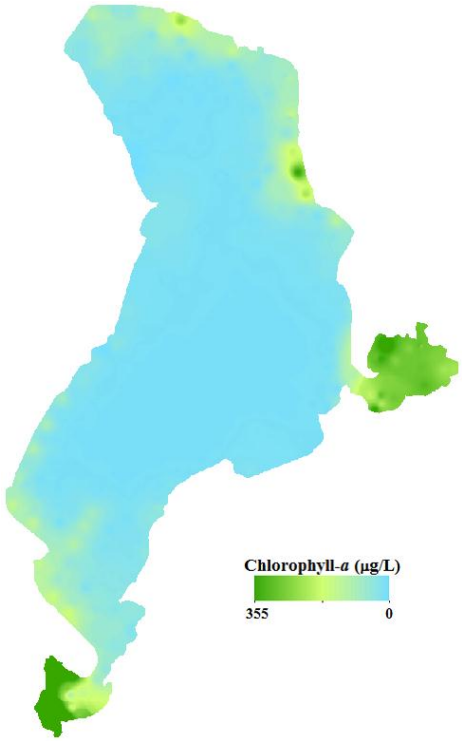

Figure 4-13: Chlorophyll-*a* mapping over Utah Lake for summer 2008

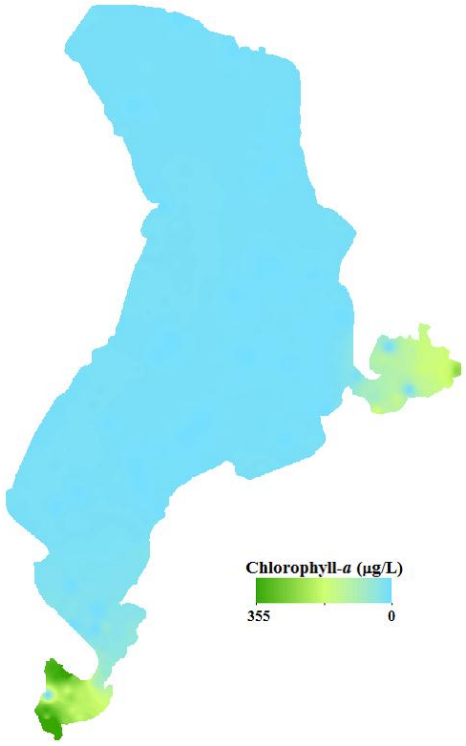

Figure 4-14: Chlorophyll-*a* mapping over Utah Lake for summer 2009

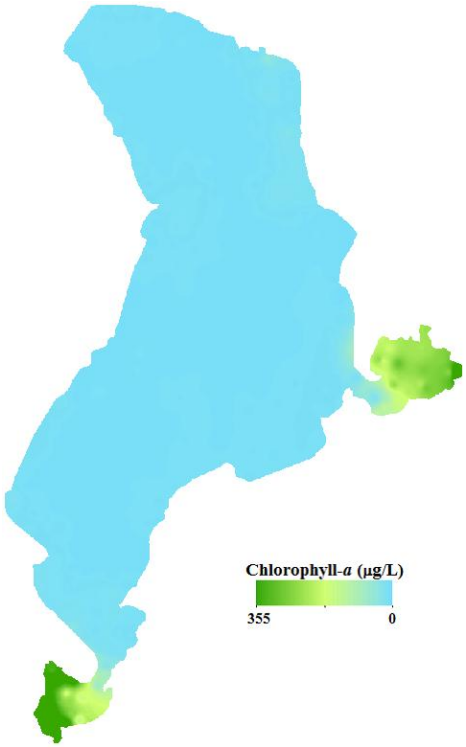

Figure 4-15: Chlorophyll-*a* mapping over Utah Lake for summer 2010

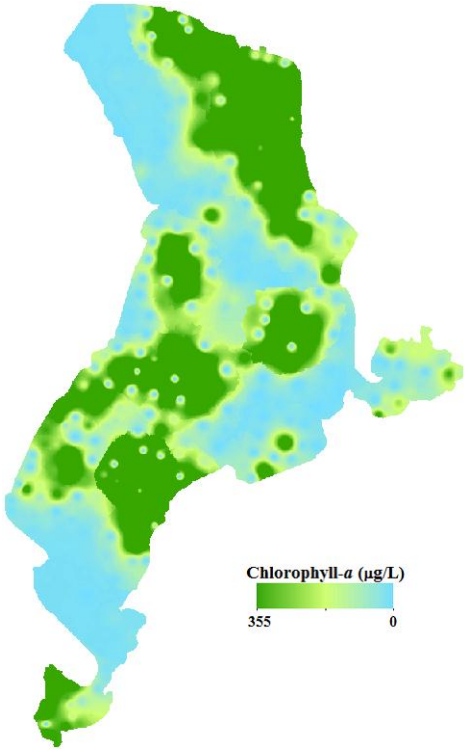

Figure 4-16: Chlorophyll-*a* mapping over Utah Lake for fall 2006

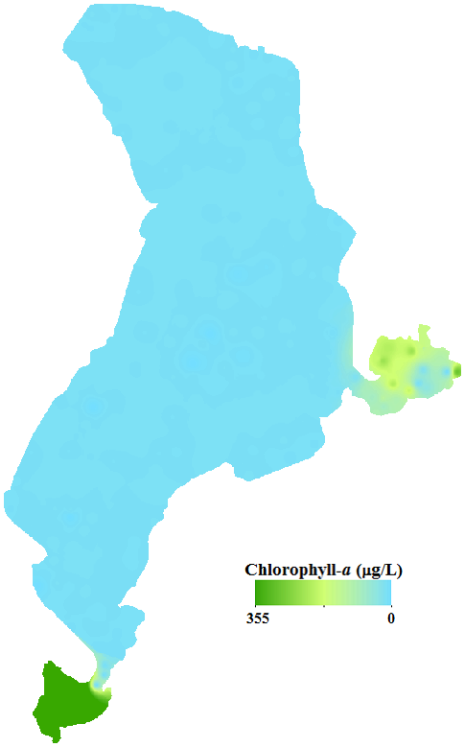

Figure 4-17: Chlorophyll-*a* mapping over Utah Lake for fall 2007

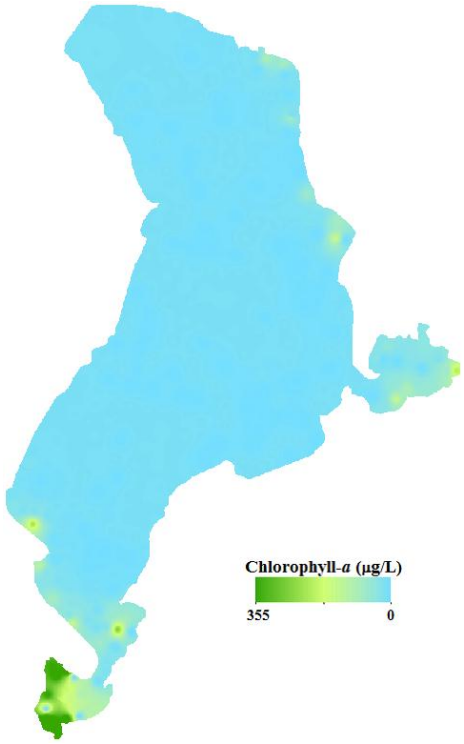

Figure 4-18: Chlorophyll-*a* mapping over Utah Lake for fall 2009

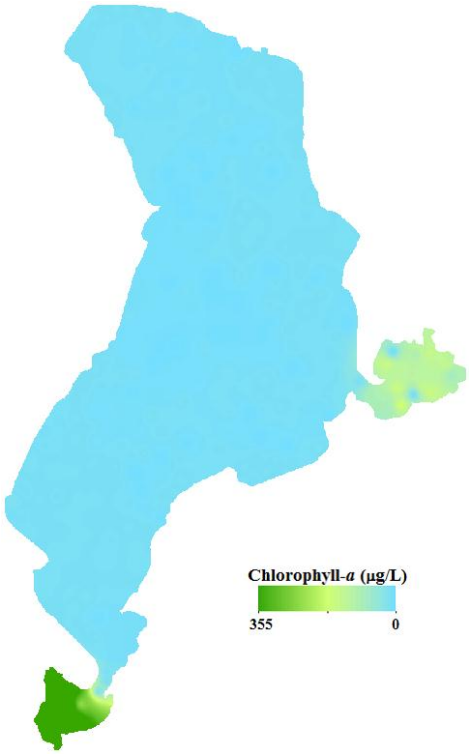

Figure 4-19: Chlorophyll-*a* mapping over Utah Lake for fall 2010

4.2 Correlation and Trend

Figure 4-20 shows the correlation between the total phosphorus concentrations (field measurement for July 6 and September 17, 2009), and the chlorophyll-*a* concentrations (model estimates for July 8 and September 26, 2009). From the plot it was established that phosphorus has a high correlation with chlorophyll-*a* ($R^2 = 0.9046$).

The plot shown in Figure 4-21 illustrates the average chlorophyll-*a* concentration for all the 370 pixel data points. This average concentration has been used to represent the concentration of chlorophyll-*a* for the entire lake. This data plot is to help show the overall trend of chlorophyll-*a* over time.

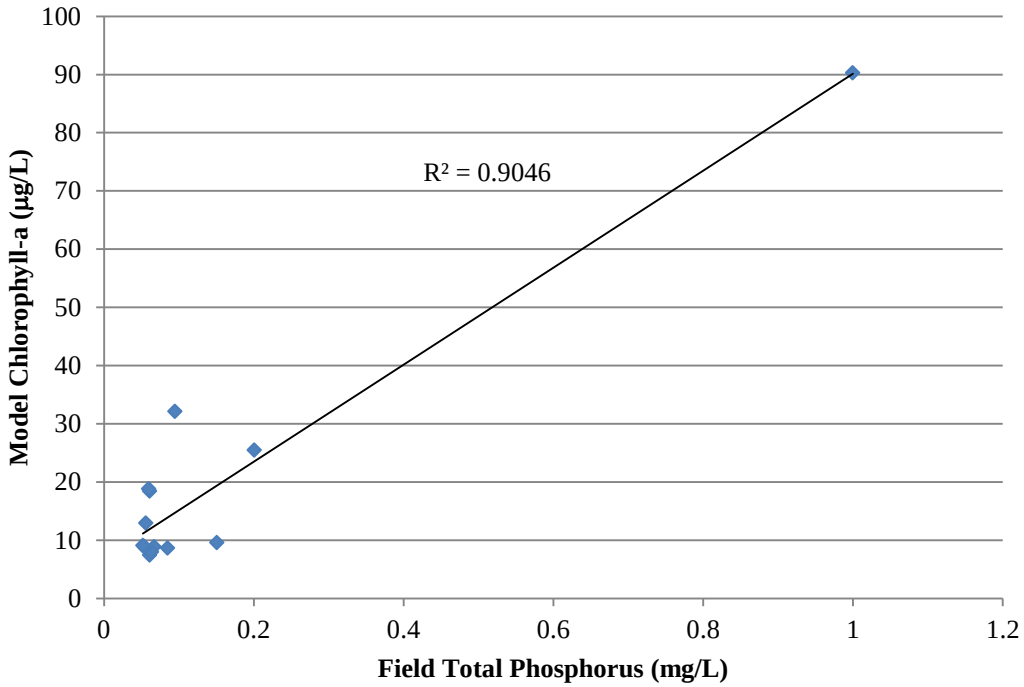

Figure 4-20: Correlation between concentrations of total phosphorus (field) and chlorophyll-*a* (model)

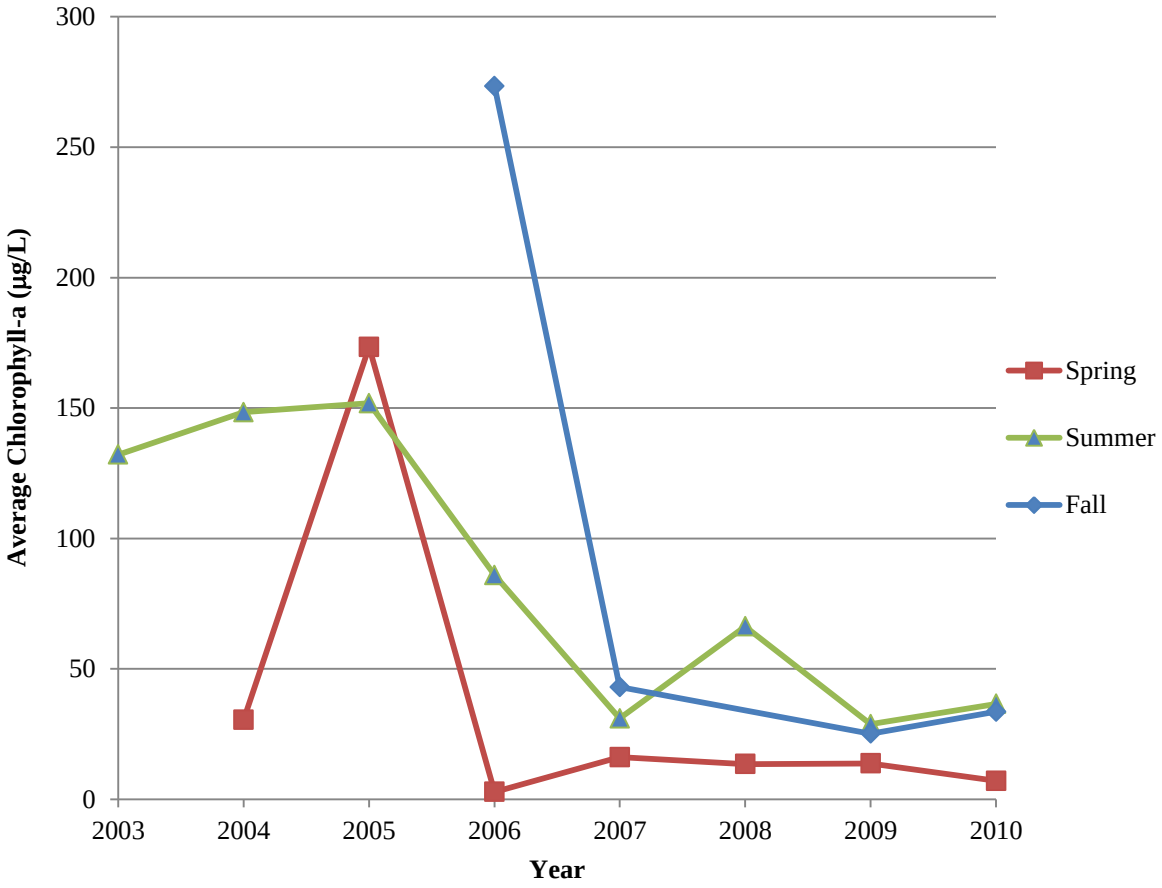

Figure 4-21: Average chlorophyll-*a* concentration for Utah Lake

5 DISCUSSION

From 2003 to 2010, the contour maps reveal that the maximum values for chlorophyll-*a* concentration occurred mostly at the southern (Goshen Bay) and eastern (Provo Bay) sections of Utah Lake. Other sections of the lake exhibited colorings that indicated chlorophyll-*a* concentrations of 20µg/L and lower.

However, in the summer and fall of 2006, the middle, western, and north-eastern sections of the lake also exhibited high levels of chlorophyll (355µg/L and higher). In the summer of 2005, about 90% of the lake showed color mappings that indicated concentrations less than 120µg/L.

In spring 2005, there was a marked increase in chlorophyll-*a* concentrations at the north-eastern, eastern, south-eastern, and southern ends of the lake. These portions showed concentrations of 355µg/L and higher. This could be as a result of the point discharges from storm drains, waste water treatment plants, and non point runoff from agricultural and pastoral lands. The locations of the point and non-point sources can be seen in Figure 5-1.

Figure 5-1 illustrates the various treatment plants and storm drains that discharge wastewater directly into the lake or indirectly via Utah Lake's tributaries. The wastewater sources are from the municipal and industrial activities in Utah Lake's neighboring towns. Major sources of problematic wastewater include: wastewater treatment plants in Springville, Provo, Orem, Spanish Fork, Timpanogos, Payson; and the drains from Geneva Steel and Steel Mill.

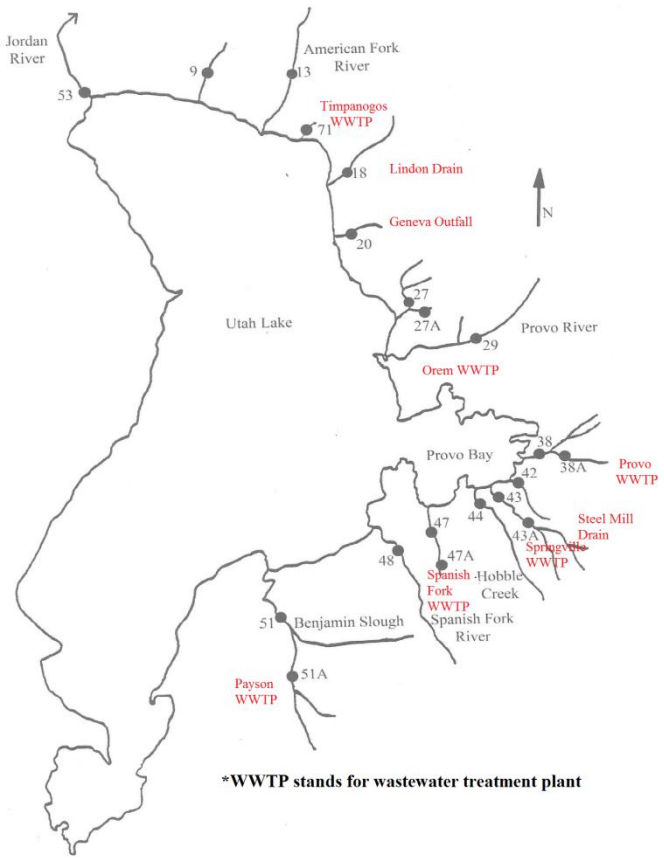

Figure 5-1: Wastewater treatment plants and other sources of wastewater discharge into Utah Lake

It has been previously established in this report that chlorophyll-*a* and phosphorus are highly correlated. Although determining the exact concentrations of phosphorus in Utah Lake using remote sensing methods is beyond the scope of this study, the use of chlorophyll-*a* contour maps generated using Landsat 7 ETM+ imagery is a good indication of which sections of the lake have high or low phosphorus concentrations. For example, the apparently high concentrations of chlorophyll-*a* at the Provo Bay area is an indication of high concentrations of phosphorus at that location.

With the exception of the sharp increase in chlorophyll-*a* concentration in spring 2005, there has been a general decline in chlorophyll-*a* concentration over time for spring, summer,

and fall. In spring, the Lake average chlorophyll-*a* concentration reduced from 30.51µg/L in 2004 to 7.08µg/L in 2010. In summer, this average reduced from 132.13µg/L in 2003 to 36.58µg/L in 2010. Finally, in fall, the Lake average chlorophyll-*a* concentration reduced from 273.40µg/L in 2006 to 33.59µg/L in 2010.

6 CONCLUSION

This study shows that ln(Band 3/Band 4) or the log transformation of the red/near-infrared reflectance ratio is a good predictor of chlorophyll-*a* concentration in a turbid lake such as Utah Lake. There was a strong correlation between concentrations of phosphorus and chlorophyll-*a*. This suggests that the spatial and temporal distribution of chlorophyll-*a* over Utah lake is helpful in locating areas with high or low phosphorus concentrations.

The model estimates for 2003 to 2010 suggests a decline in the average chlorophyll-*a* concentration in Utah Lake for the seasons under study (spring, summer, and fall seasons). Generally about 90% of the Lake area had chlorophyll-*a* concentrations lower than 20µg/L. High concentrations of Chlorophyll-*a* (355µg/L and over) were observed mostly at the Provo Bay and Goshen Bay areas of the Lake. Occasionally, elevated levels of chlorophyll-*a* were observed at the northeastern, middle, and western sections of the lake. This suggests maximum concentrations of phosphorus at the same area. This implies that the elevated levels of chlorophyll-*a* might be a result of the point and non-point discharge of phosphorus-laden wastewater from treatment plants, municipal storm drains, and agricultural activities.

REFERENCES

Apha, A. "Wef, Standard Methods for the Examination of Water and Wastewater." *American Public Health Association, Washington, DC* (1995).

Bartholomew, P. "Mapping and Modeling Chlorophyll-*a* Concentrations in the Lake Manassas Reservoir Using Landsat Thematic Mapper Satellite Imagery." Virginia Polytechnic Institute and State University, 2002.

Carlson, R.E. "A Trophic State Index for Lakes." *Limnology and Oceanography* 22, no. 2 (1977): 361-369.

Dekker, A.G., T.J. Malthus, and E. Seyhan. "Quantitative Modeling of Inland Water Quality for High-Resolution Mss Systems." *Geoscience and Remote Sensing, IEEE Transactions on* 29, no. 1 (1991): 89-95.

Dekker, AG, TJ Malthus, and HJ Hoogenboom. "The Remote Sensing of Inland Water Quality." *Advances in Environmental Remote Sensing* (1995): 123–142.

Gitelson, A., M. Mayo, YZ Yacobi, A. Parparov, and T. Berman. "The Use of High-Spectral-Resolution Radiometer Data for Detection of Low Chlorophyll Concentrations in Lake Kinneret." *Journal of plankton research* 16, no. 8 (1994): 993.

Han, L. "Spectral Reflectance with Varying Suspended Sediment Concentrations in Clear and Algae-Laden Waters." *Photogrammetric engineering and remote sensing* 63, no. 6 (1997): 701-705.

Han, L., and D.C. Rundquist. "Comparison of Nir/Red Ratio and First Derivative of Reflectance in Estimating Algal-Chlorophyll Concentration: A Case Study in a Turbid Reservoir." *Remote Sensing of Environment* 62, no. 3 (1997): 253-261.

Harding, LW, EC Itsweire, and WE Esaias. "Algorithm Development for Recovering Chlorophyll Concentrations in the Chesapeake Bay Using Aircraft Remote Senging, 1989-91." *Photogrammetric engineering and remote sensing* 61, no. 2 (1995): 177-185.

Kirk, JTO. "Light and Photosynthesis in Aquatic Ecosystems, 401 Pp." Cambridge Univ. Press, New York, 1983.

Mittenzwey, K.H., S. Ullrich, AA Gitelson, and KY Kondratiev. "Determination of Chlorophyll a of Inland Waters on the Basis of Spectral Reflectance." *Limnology and Oceanography* (1992): 147-149.

Pimentel, D., C. Harvey, P. Resosudarmo, K. Sinclair, D. Kurz, M. McNair, S. Crist, L. Shpritz, L. Fitton, and R. Saffouri. "Environmental and Economic Costs of Soil Erosion and Conservation Benefits." *Science* 267, no. 5201 (1995): 1117.

PSOMAS. *Utah Lake Tmdl Final Draft*. 2007.

Quibell, G. "The Effect of Suspended Sediment on Reflectance from Freshwater Algae." *International Journal of Remote Sensing* 12, no. 1 (1991): 177-182.

Ritchie, J.C., P.V. Zimba, and J.H. Everitt. "Remote Sensing Techniques to Assess Water Quality." *Photogrammetric engineering and remote sensing* 69, no. 6 (2003): 695-704.

Wetzel, R.G. *Limnology: Lake and River Ecosystems*. Vol. 1006: Academic press San Diego, CA, 2001.

Yu, K.P., J. Yoon, and B.K. Muhammad. "Developing a Monitoring Support Model for Chlorophyll a Concentration in the James River Estuary Using Modis Images." ASCE, 2007.

APPENDIX A. OTHER BAND REFLECTANCE MODELS

The following band relationships where used to generate model equations for chlorophyll-*a* concentrations, however, due to poor correlation and/or models not matching the physical process, these equations where not considered to be good predictors of chlorophyll-*a* in a turbid waterbody such as Utah Lake. The figures below show a plot of field measured chlorophyll-*a* (June 22 and July 6, 2009) versus Landsat (June22 and July 8, 2009) Band 3/Band 4 reflectance ratios.

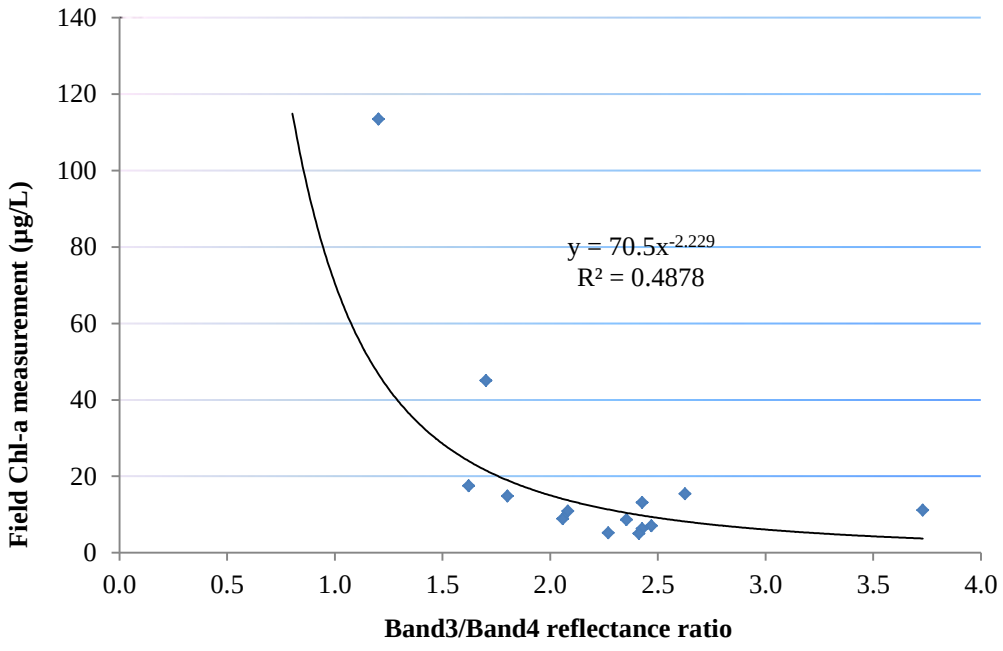

Figure A-1: Field measured chlorophyll-*a* vs. Band 3/Band 4 (power trendline)

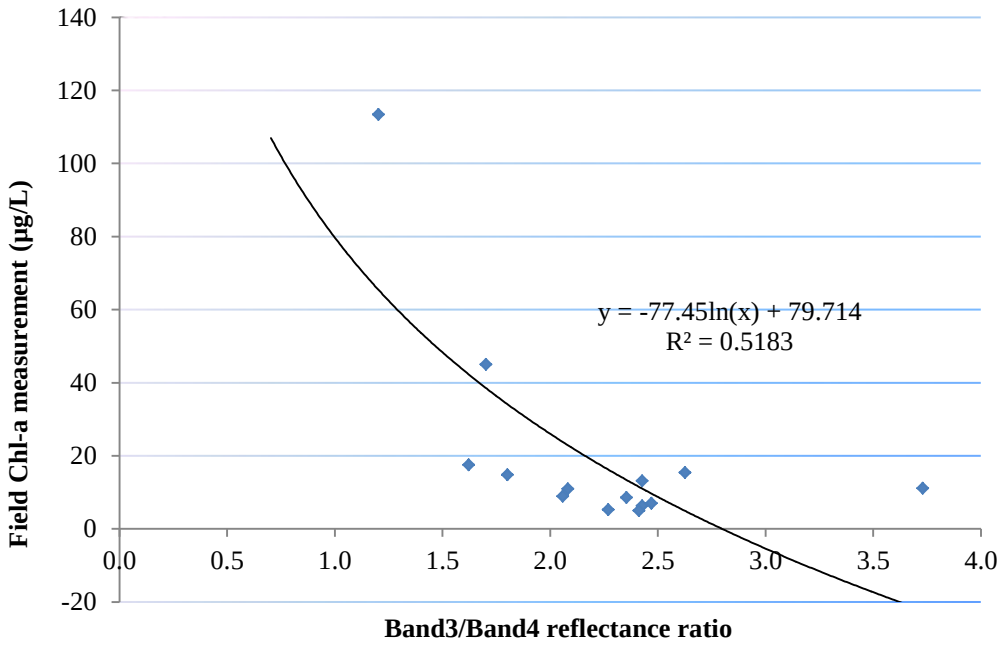

Figure A-2: Field measured chlorophyll-*a* vs. Band 3/Band 4 (logarithmic trendline)

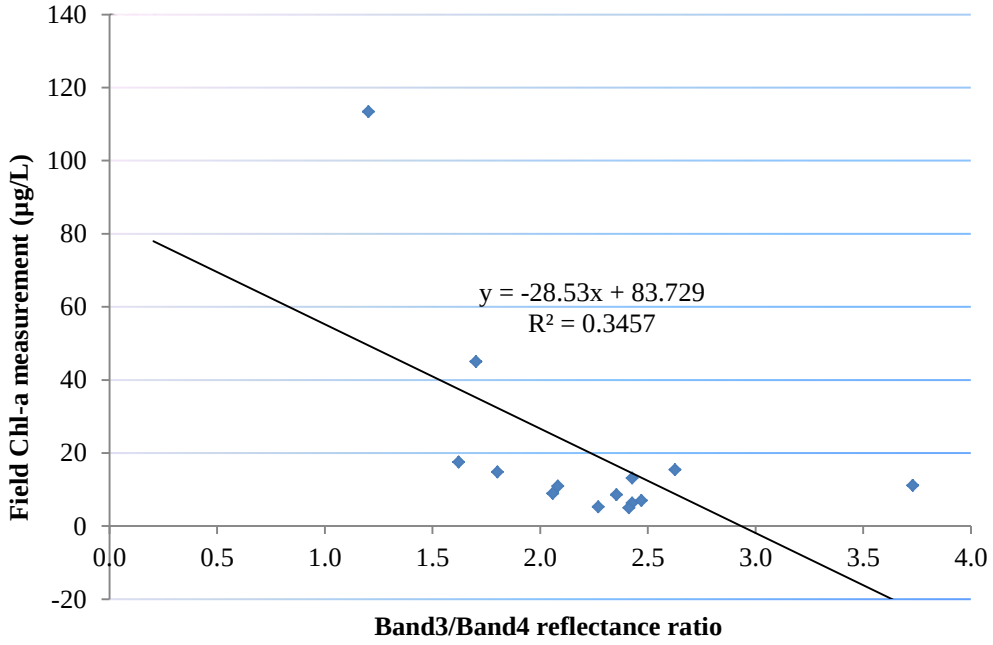

Figure A-3: Field measured chlorophyll-*a* vs. Band 3/Band 4 (linear trendline)

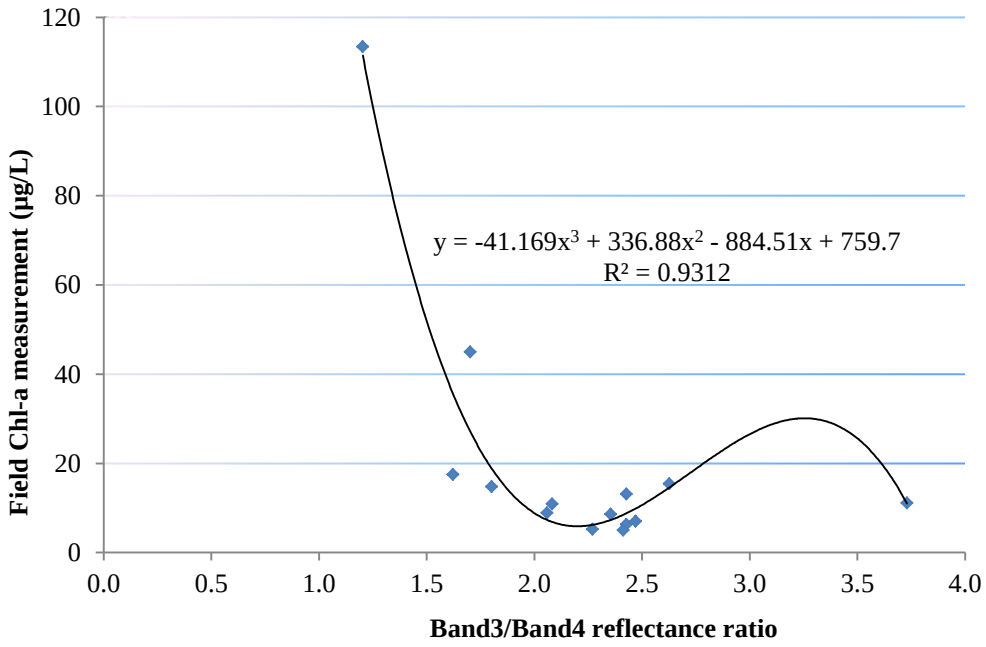

Figure A-4: Field measured chlorophyll-*a* vs. Band 3/Band 4 (polynomial trendline)

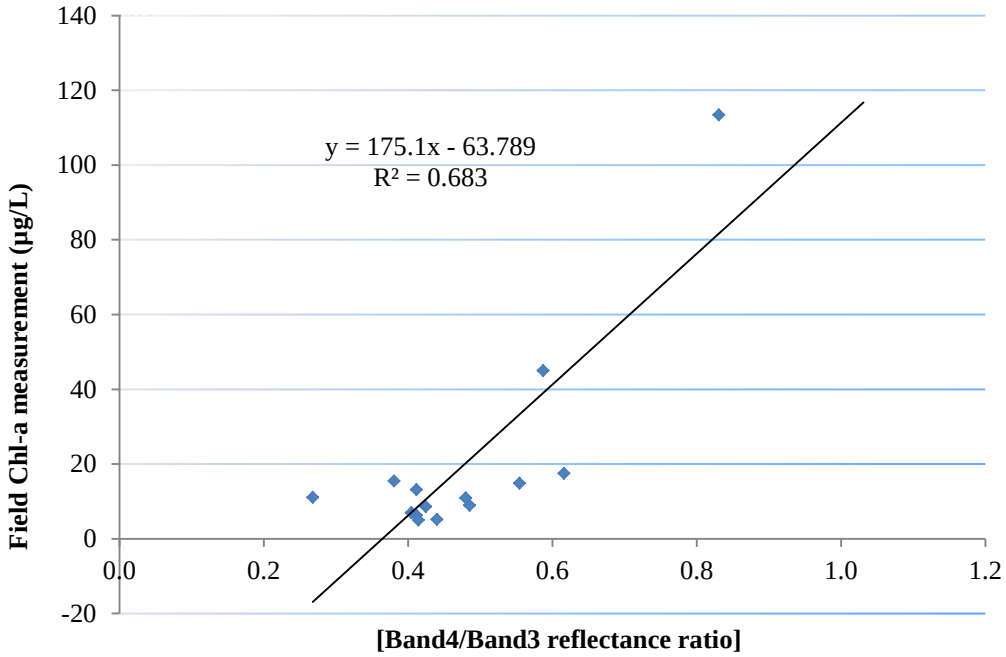

Figure A-5: Field measured chlorophyll-*a* vs. Band 4/Band 3 (linear trendline)

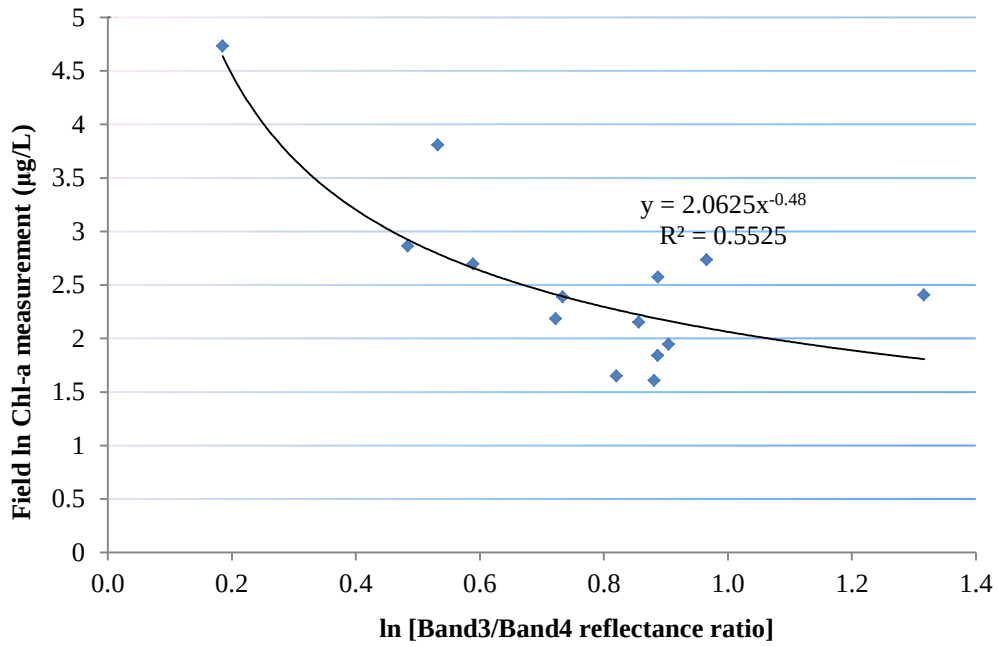

Figure A-6: ln chlorophyll-*a* vs. ln[Band 3/Band 4] (power trendline)

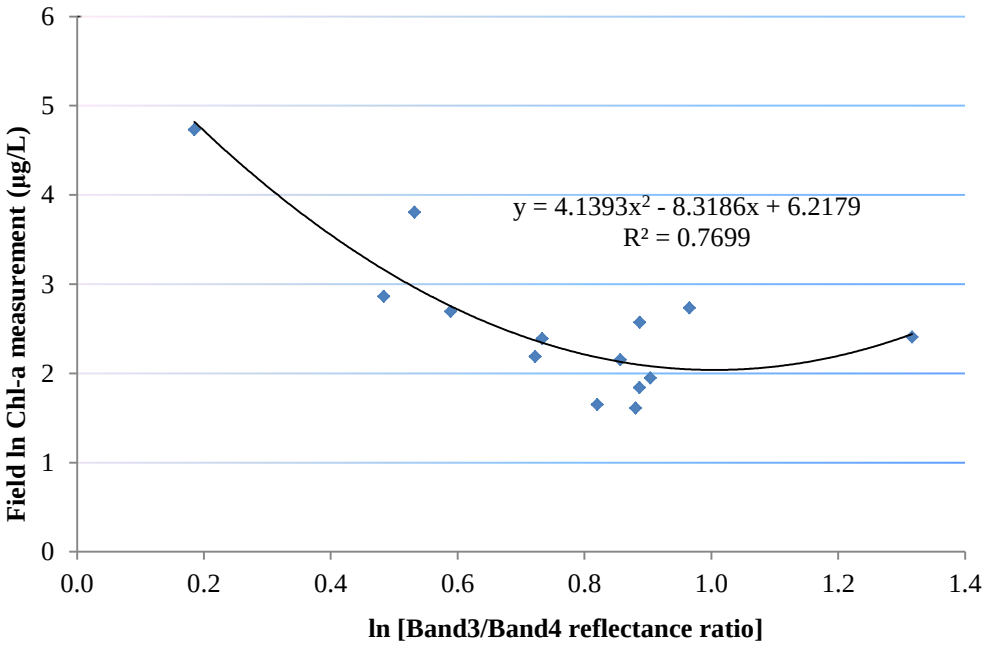

Figure A-7: ln chlorophyll-*a* vs. ln[Band 3/Band 4] (polynomial trendline)

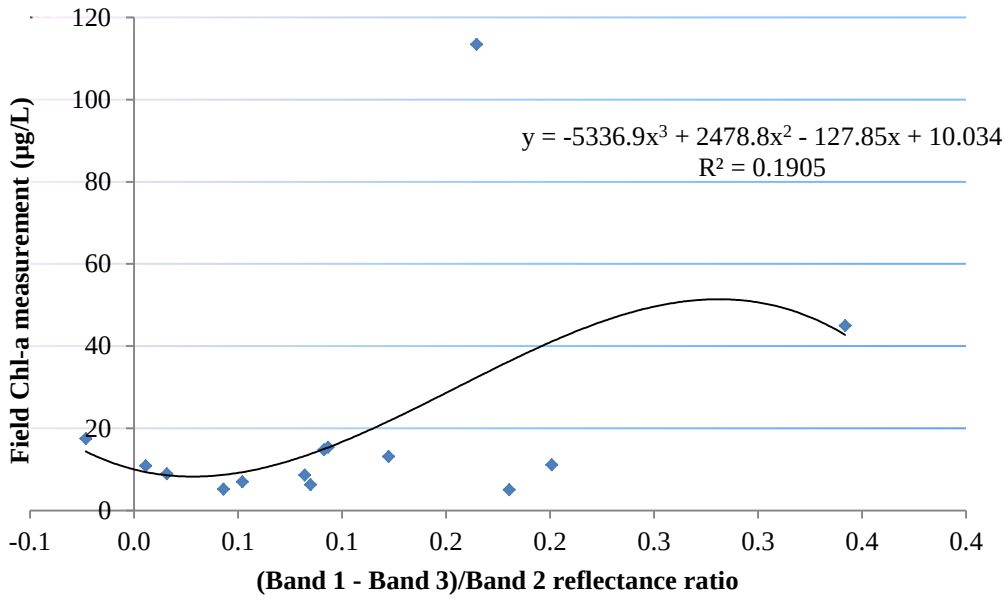

Figure A-8: Field measured chlorophyll-*a* vs. (Band 1 – Band 3)/Band 2 (polynomial trendline)

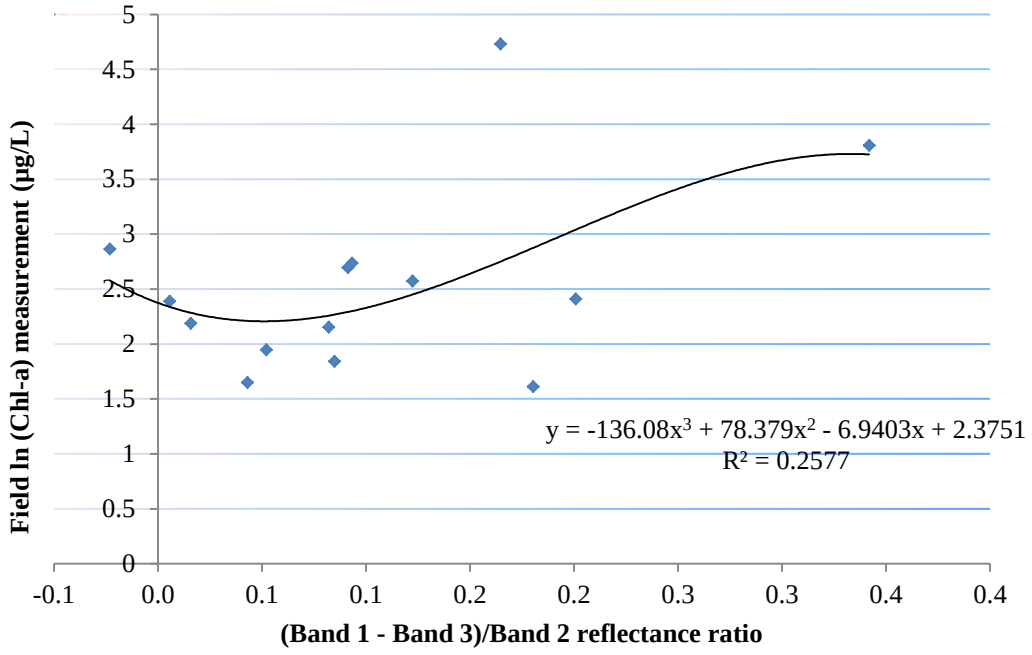

Figure A-9: ln[chlorophyll-*a*] vs. (Band 1 – Band 3)/Band 2 (polynomial trendline)

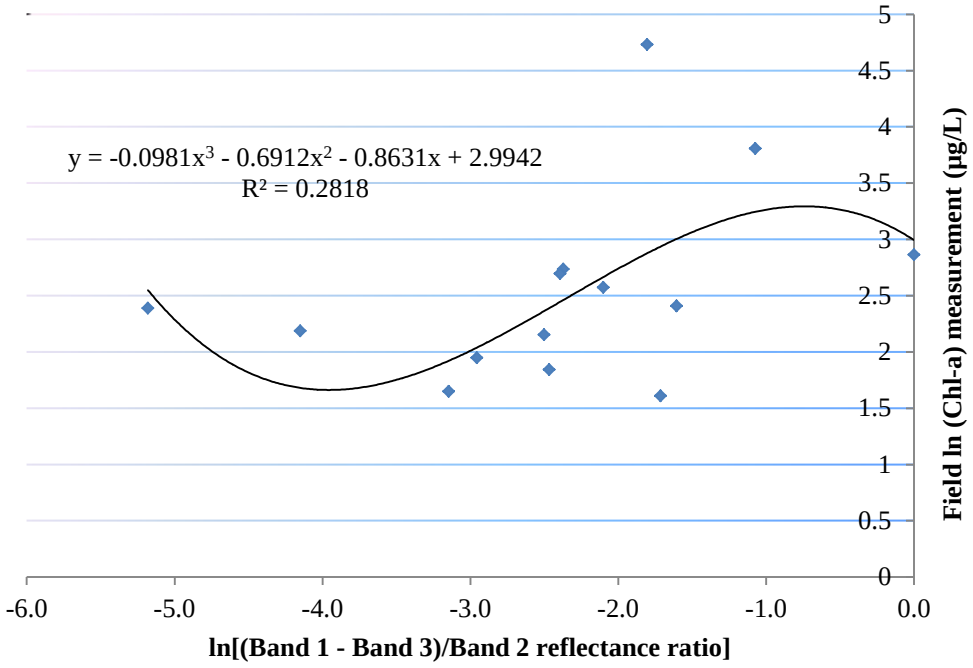

Figure A-10: ln chlorophyll-*a* vs. ln (Band 1 – Band 3)/Band 2 (polynomial trendline)

APPENDIX B. LANDSAT CALIBRATION

The following equations and explanation for ENVI Landsat calibration were sourced from ENVI 4.7 help file. ENVI uses the following equations to convert digital numbers to radiance and exoatmospheric reflectance (ρ_p):

$$\rho_p = \frac{\rho \cdot L_\rho \cdot d^2}{ESUN_\rho \cdot \cos(\rho_s)} \quad \text{(B-1)}$$

where:

- L_λ is the spectral radiance
- d is the Earth-Sun distance in astronomical units
- $ESUN_\lambda$ is the mean solar exoatmospheric irradiance. (ENVI uses the $ESUN_\lambda$ values from the Landsat 7 Science Data Users Handbook for Landsat 7 ETM+)
- θ_s is the solar zenith angle in degrees

The spectral radiance L_λ is calculated in ENVI using the following equation:

$$L_\lambda = LMIN_\lambda + \left(\frac{LMAX_\lambda - LMIN_\lambda}{QCALMAX - QCALMIN}\right)(QCAL - QCALMIN) \quad \text{(B-2)}$$

where:

- QCAL is the calibrated and quantized scaled radiance in units of digital numbers
- $LMIN_\lambda$ is the spectral radiance at QCAL = 0
- $LMAX_\lambda$ is the spectral radiance at QCAL = QCALMAX

  $LMIN_\lambda$ and $LMAX_\lambda$ are derived from values published from Chander, Markham, and Helder (2009).
- QCALMIN is the minimum quantized calibrated pixel value (corresponding to $LMIN_\lambda$) in DN. Valid values are as follows:

  1: LPGS products

  1: NLAPS products processed after 04 April 2004

  0: NLAPS products processed before 05 April 2004

  When metadata is not available to determine the appropriate values, QCALMIN is set by default to 1 (TM and ETM+) or 0 (MSS).
- QCALMAX is the maximum quantized calibrated pixel value (corresponding to $LMAX_\lambda$) in DN. Valid values are 127, 254, or 255. When metadata is not available to determine the appropriate values, QCALMAX is set by default to 255 (TM and ETM+) or 127 (MSS).

The resulting radiance (L_λ) is in units of watts per square meter per steradian per micrometer ($W/(m^2 \cdot sr \cdot \mu m)$).